DFT Study on the Mechanisms of Stereoselective C(2)-Vinylation of 1-Substituted Imidazoles with 3-Phenyl-2-propynenitrile

Donghui Wei and Mingsheng Tang*

Department of Chemistry, Center of Computational Chemistry, Zhengzhou University, Zhengzhou, Henan, 450052

Received: May 22, 2009; Revised Manuscript Received: August 15, 2009

Recently, the first examples of direct vinylation of 1-substituted imidazoles at the 2-position of the imidazole nucleus have been described (*J. Org. Chem.* **2008**, *73*, 9155−9157). 1-Substituted imidazoles are *C*(2)-vinylated with 3-phenyl-2-propynenitrile at room temperature without catalyst and solvent to afford 3-(1-organyl-1*H*-imidazol-2-yl)-3-phenyl-2-propenenitriles, mainly (ca. 95%) as (*Z*)-isomers, in 56−88% yield. Nevertheless, the stereoselectivity of vinylation, which has been elusive over the past decades, is still a big problem to explain. In this paper, the reaction mechanisms of stereoselective C(2)-vinylation of 1-methylimidazole with 3-phenyl-2-propynenitrile have been investigated using density functional theory (DFT). The geometries of the reactants, transition states, intermediates, and products were optimized at the B3LYP/6-31G(d,p) level. The calculated results reveal that the reaction contains three processes: formation of zwitterion, proton transfer, and ring rearrangement. Four possible reaction channels are shown, including two (*E*)-isomer channels and two (*Z*)-isomer channels. One of the (*Z*)-isomer channels has the lowest energy barrier among all the four channels, with the highest energy barrier for 83.62 kJ/mol, so it occurs more often than the others at room temperature, which is in good agreement with experiment. Further calculations of solvation effects show that the title reaction can be carried out more smoothly in the gas phase.

Introduction

Recently, the first examples of direct vinylation of 1-substituted imidazoles at the 2-position of the imidazole nucleus have been described by Trofimov and co-workers;[1] understanding the unexpected stereoselectivity which has initiated this computational study should be meaningful for the imidazole chemistry. Imidazoles are one kind of common scaffold in highly significant biomolecules, including biotin, the essential amino acid histidine, histamine, the pilocarpine alkaloids,[2] and other alkaloids, which have been shown to exhibit interesting biological activities such as antimicrobial and anticryptococcal.[3] Imidazole derivatives have also been found to possess many pharmacological properties and are widely implicated in biochemical processes.[4−8]

Due to the wide-ranging applications of imidazoles in organic and medicinal chemistry, more and more attention has been paid to seeking variously functionalized imidazoles. Therefore, the development of synthetic methodologies has been, and continues to be, an area of interest in organic chemistry.[9−16] There has already been much effort in designing and developing various types of imidazoles experimentally.[1,17−31] For example, McNab et al. synthesized 2-vinylimidazoles having ester and cyano functions in the vinyl group from 1*H*-imidazole-2-carbaldehyde and active methylene compounds.[20] Gusarova and co-workers reported that 1-organyl-2-formylimidazoles and -benzimidazoles reacted with diorganylphosphine oxides under mild conditions (room temperature, dioxane, 1 h) to give, in practically quantitative yields, 2-(diorganylphosphorylhydroxymethyl)-1-organylimidazoles.[22]

It is noteworthy that Trofimov et al. found zwitterionic adducts to be common for the reactions of α,β-acetylenic γ-hydroxy nitriles with pyridines,[26,27] quinoline and quinoxaline,[28] phenanthridines,[29] natural alkaloid (anabasine),[30] and 1-substituted benzimidazoles;[31] but the stereoselectivity of vinylation, which had been elusive over the past decades, was unexplained in these papers. In addition, they had also reported the first examples of direct vinylation of 1-substituted imidazoles at the 2-position of the imidazole nucleus. 1-Substituted imidazoles are *C*(2)-vinylated with 3-phenyl-2-propynenitrile at room temperature without catalyst and solvent to afford 3-(1-organyl-1*H*-imidazol-2-yl)-3-phenyl-2-propenenitriles, mainly (ca. 95%) as (*Z*)-isomers, in 56−88% yield.[1] However, as shown in Scheme 1, it seems to be impossible to make clear how the carbine intermediate (**Z**)**-M5** is generated, and so it is still a big problem to understand why the reaction can happen and why the main product is the (*Z*)-isomer rather than the (*E*)-isomer.

In this project, the compounds **R1** (1-methylimidazole, structure shown in Scheme 1) and **R2** (3-phenyl-2-propynenitrile, structure shown in Scheme 1) have been chosen as the objects of investigation, and the reaction mechanisms in the different reaction channels were studied using density functional theory, which has been widely used in the study of the mechanism.[32]

Computational Details

All theoretical calculations were performed using the *Gaussian 03*[33] suite of programs. All structures were optimized at the B3LYP/6-31G(d,p) level.[34,35] Vibrational frequency calculations were then performed at the optimized geometry of each reactant, product, transition state, and intermediate. We confirmed that all the reactants and intermediates have no imaginary frequencies, and each transition state has one, and only one, imaginary frequency. The intrinsic reaction coordinate (IRC) calculations, at the same level of theory, were performed to ensure that the transition states led to the expected reactants and products.[36,37] Additionally, we have computed single-point energies of all the

* Corresponding author. Mingsheng Tang, email: mstang@zzu.edu.cn.

10.1021/jp9047874 CCC: $40.75
Published on Web 09/17/2009

SCHEME 1

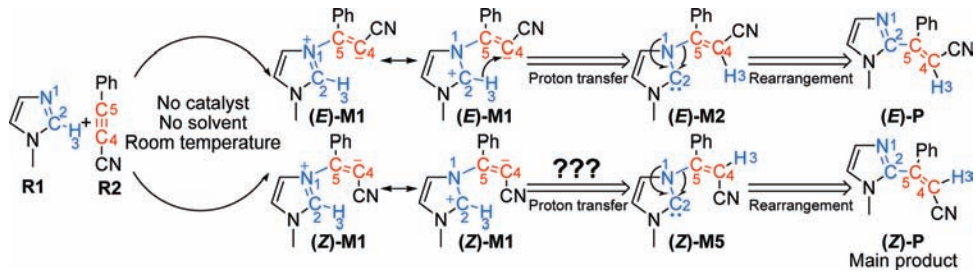

SCHEME 2: (*E*)-Isomer Mechanisms

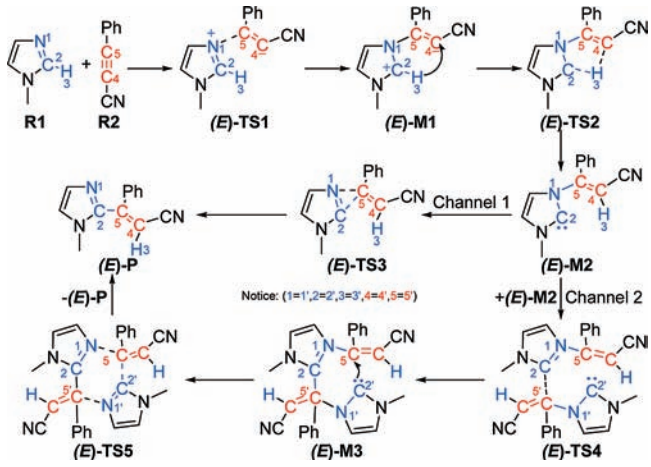

optimized stationary points in the water, ethanol, DMSO, THF, and CCl_4 solvents at the B3LYP/6-31G(d,p) level in the polarized continuum model (PCM).[38,39]

Results and Discussion

In this paper, we suggested and undertook calculations using the Gaussian program to investigate four possible reaction channels, including two (*E*)-isomer reaction channels (channel 1 and channel 2) and two (*Z*)-isomer reaction channels (channel 3 and channel 4), and the processes could be illustrated as follows:

1. (*E*)-Isomer Reaction Channels. As can be seen from Scheme 2, the -Ph group and the -CN group are in the same side of the C═C bond, so all the intermediates, transition states, and products are (*E*)-isomers in the two channels, and both reaction channel 1 and reaction channel 2 are (*E*)-isomer reaction channels.

1.1. Reaction Channel 1. There are three steps in the reaction channel 1 (Scheme 2): initially, the reactant **R1** (1-methylimidazole) forms one new bond with electron-deficient alkyne **R2**, and the (*E*)-isomer zwitterion (***E***)-**M1** is generated in this step. As shown in Figure 1, the N1−C5 bond length shortens from 1.831 Å in (*E*)-**TS1** to 1.491 Å in (***E***)-**M1**, which indicates that the N1−C5 bond has formed in (***E***)-**M1** via (***E***)-**TS1**. Simultaneously, the (*E*)-isomer is generated in (***E***)**-TS1**, and the dihedral angel of C6−C5−C4−C7 is 1.95°. The energy (all the energies in this paper are electronic energies) of (***E***)**-TS1** lies 101.47 kJ/mol (Figure 2) above that of the reactants (**R1** and **R2**), which is not a low energy barrier at room temperature.

As can be seen from Table 1, the values of charge on N1 and C5 atoms from reactants to the zwitterion **(*E*&*Z*)-M1** changed drastically, which was mainly due to the new N1−C5 bond formation. Apart from the above, the charge values of C2 atom change from 0.175 e in **R1** to 0.265 e in (***E***)-**M1** and 0.271 e in (***Z***)-**M1**, which indicates that the C2 atom becomes a positive charge center in the (***E***&***Z***)-**M1**. At the same time, the C4 atom becomes a negative charge center in the (***E***&***Z***)-**M1**; thus, the intermediates (***E***)-**M1** and (***Z***)-**M1** should be zwitterions. In addition, the charge values of H3 atom have been more positive in the zwitterions, so the H3 atom can attack the negative charge center more easily.

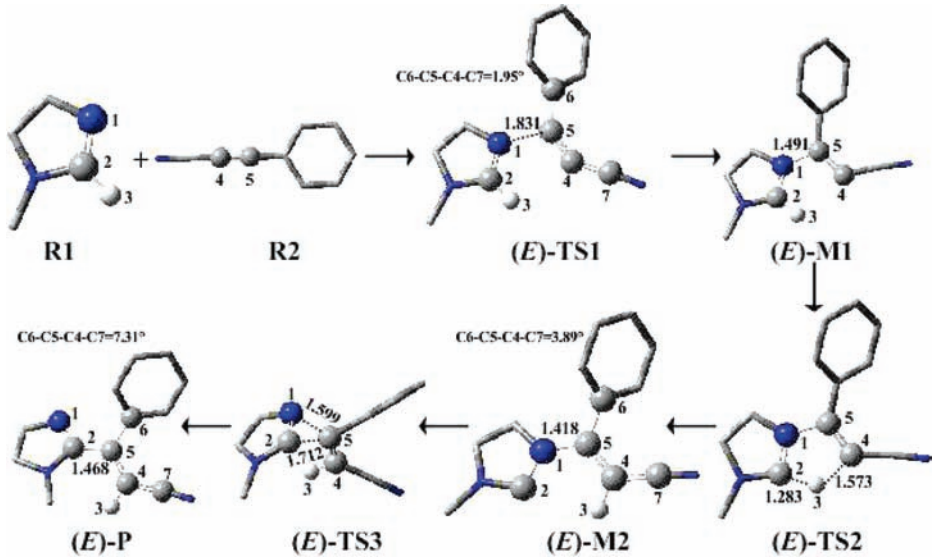

Figure 1. Structures and geometrical parameters of the reactants, (*E*)-intermediates, (*E*)-transition states, and (*E*)-product optimized at the B3LYP/6-31G(d,p) level in channel 1 (bond length in Å).

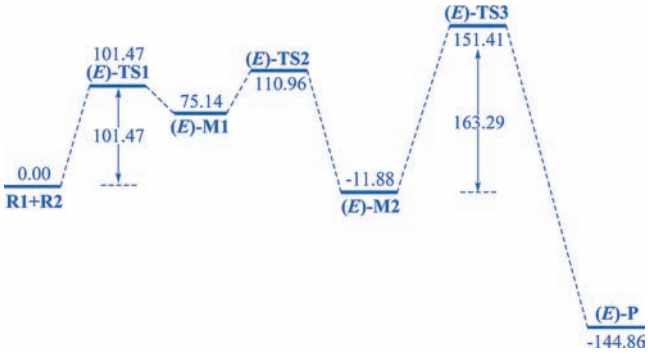

Figure 2. Energy profile of channel 1 (unit: kJ/mol).

TABLE 1: Values of NBO Charge on the N1, C2, H3, C4, and C5 Atoms in R1, R1, (*E*)-M1, and (*Z*)-M1 at the B3LYP/6-31G(d,p) Level (unit: e)

	N1	C2	H3	C4	C5
R1	−0.496	0.175	0.219	—	—
R2	—	—	—	−0.125	0.119
(*E*)-**M1**	−0.325	0.265	0.288	−0.358	0.039
(*Z*)-**M1**	−0.351	0.271	0.280	−0.291	0.031

The second step is a proton transfer reaction, after which the carbene intermediate (*E*)-**M2** forms via (*E*)-**TS2**. In (*E*)-**TS2**, the bond lengths of C2−H3 and H3−C4 are 1.283 and 1.573 Å, so it can be seen that the H3 atom transfers from the C2 atom in (*E*)-**M1** to the C4 atom in (*E*)-**M2**. It is noteworthy that, since the N1−C2 bond and C4−C5 bond are conjugative and the N1, C2, H3, C4, and C5 atoms are in the same plane in (*E*)-**TS2**, it seems to be impossible to obtain a (*Z*)-isomer via this step.

The last step of reaction channel 1 is a three-membered ring rearrangement process. In (*E*)-**TS3**, the bond lengths of N1−C5 and C2−C5 are 1.599 and 1.712 Å, so we can see that the N1−C5 bond in (*E*)-**M2** breaks and the C2−C5 bond in (*E*)-**P** generates via (*E*)-**TS3**. Moreover, the dihedral angel of C6−C5−C4−C7 is 7.31°, which implies that it is also an (*E*)-isomer in the rearrangement process. However, the energy barrier of this step is so high (163.29 kJ/mol) that the reaction cannot go along at room temperature, which is mainly due to the strain in the formed three-membered ring in (*E*)-**TS3**.

1.2. Reaction Channel 2. The reaction processes of channel 2 are the same as those of channel 1 except the last rearrangement step (Scheme 2), which is a stepwise six-membered ring rearrangement process (Figure 3).

There are two (*E*)-**M2** to participate in the reaction, the C2−C5′ bond forms in (*E*)-**M3** via (*E*)-**TS4** rather than the C2−C5 bond, then the C1−C5 and C1′-C5′ bonds break and the C2′-C5 bond generates, and (*E*)-**M3** rearranges to two (*E*)-**P** via (*E*)-**TS5**. The distance of C2−C5′ changes from 1.940 Å in (*E*)-**TS4** to 1.544 Å in (*E*)-**M3**, and then the distance of C2′-C5 changes from 3.344 Å in (*E*)-**M3** to 2.112 Å in (*E*)-**TS5**; at last, both of them are 1.468 Å and the six-membered ring breaks into two (*E*)-**P**.

We set the energy of (*Z*)-**M2** (Figure 6) as 0.00 kJ/mol as a reference in this process, since the highest energy barrier of rearrangement process is only 89.25 kJ/mol (Figure 4), channel 2 is more energetically favorable than channel 1. As shown in Figure 4, the energy barrier of the first step is the highest energy barrier (101.47 kJ/mol); thus, (*E*)-**TS1** is important for kinetics of the reaction. Furthermore, the energy of product (*E*)-**P** is 144.86 kJ/mol lower than that of reactants, so the reaction is an exothermic process.

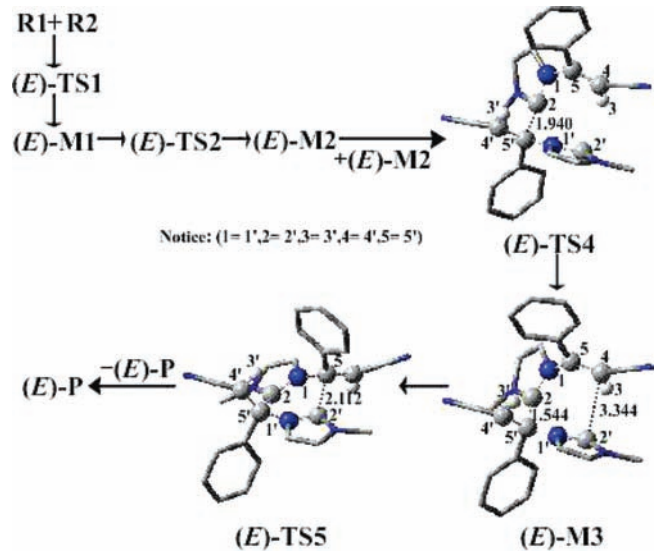

Figure 3. The structures and the geometrical parameters of the (*E*)-intermediates, (*E*)-transition states, and (*E*)-product optimized at the B3LYP/6-31G(d,p) level in channel 2 (bond length in Å).

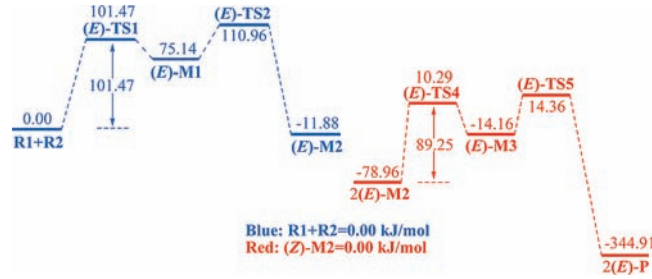

Figure 4. Energy profile of channel 2 (unit: kJ/mol).

SCHEME 3: (*Z*)-Isomer Mechanisms

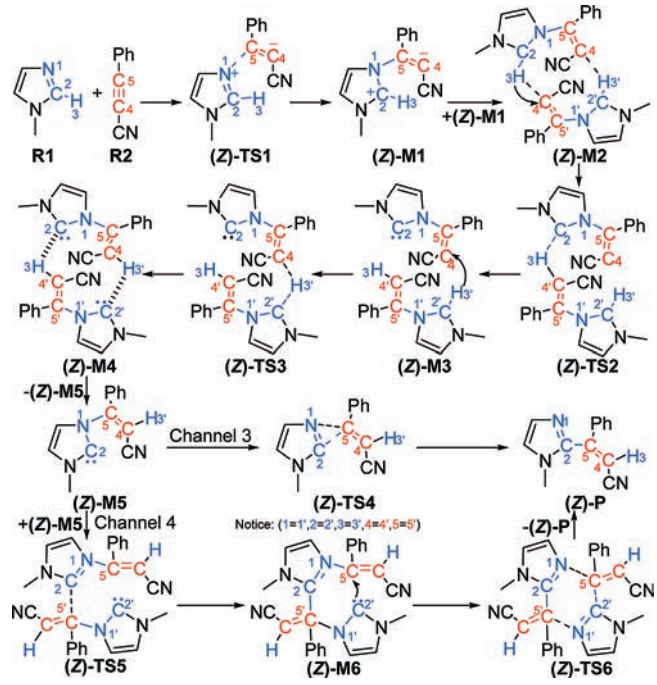

2. (*Z*)-Isomer Reaction Channels. As shown in Scheme 3, the -Ph group and -CN group are in different sides of the C═C bond, so all the intermediates and transition states are (*Z*)-isomers. There are two reaction channels, including channel 3 and channel 4, and both are (*Z*)-isomer reaction channels.

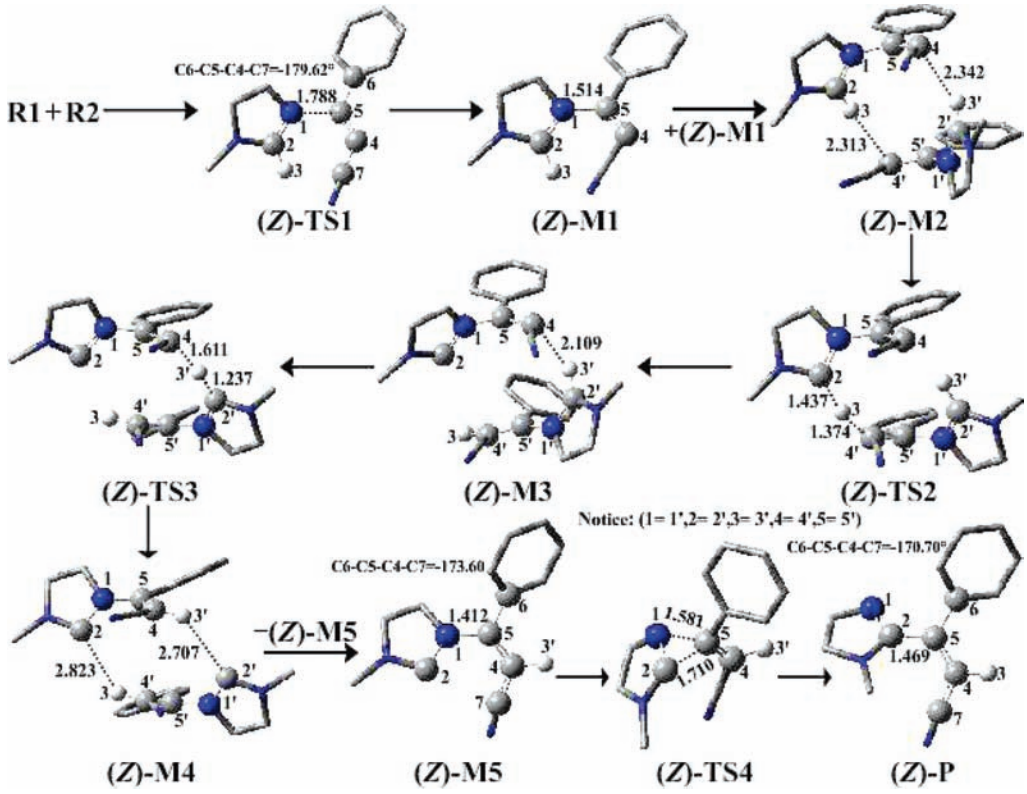

Figure 5. Structures and geometrical parameters of the (*Z*)-intermediates, (*Z*)-transition states, and (*Z*)-product optimized at the B3LYP/6-31G(d,p) level in channel 3 (bond length in Å).

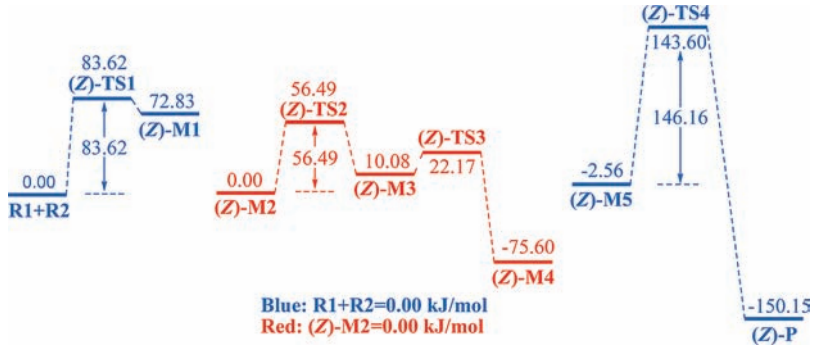

Figure 6. Energy profile of channel 3 (unit: kJ/mol).

2.1. Reaction Channel 3. Compared with the reaction channel 1, there are also three similar processes in the reaction channel 3 (Scheme 3): first, **R1** forms one new bond with **R2**, and the (*Z*)-isomer zwitterion (**Z**)-**M1** generates in this step. As shown in the Figure 5, the N1−C5 bond length shortens from 1.788 Å in (**Z**)-**TS1** to 1.514 Å in (**Z**)-**M1**, which indicates that the N1−C5 bond has formed in (**Z**)-**M1** via (**Z**)-**TS1**. Simultaneously, Z-isomer is generated in (**Z**)-**TS1**, and the dihedral angel of C6−C5−C4−C7 is −179.62°. The energy of (**Z**)-**TS1** lies 83.62 kJ/mol (Figure 6) above the reactants, which is 17.85 kJ/mol lower than that of (***E***)-**TS1**, so the (*Z*)-mechanisms are more energetically favorable than the (*E*)-channels (channel 1 and channel 2), and the reaction must generate more (*Z*)-product rather than (*E*)-product.

The following process of reaction channel 3 is a stepwise proton transfer reaction using two (**Z**)-**M1**, so we set the energy of (**Z**)-**M2** as 0.00 kJ/mol as reference in this process. In the first instance, the two (**Z**)-**M1** form the intermediate (**Z**)-**M2** by weak interaction (Figure 5), and the distances of H3−C4′ and H3′−C4 are 2.313 and 2.342 Å, separately. In the next step, the H3 atom transfers from C2 atom in (**Z**)-**M2** to C4′ atom in

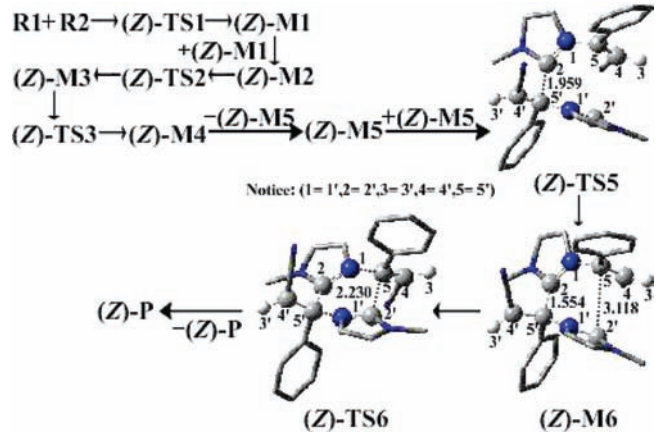

Figure 7. Structures and geometrical parameters of the (*Z*)-intermediates, (*Z*)-transition states, and (*Z*)-product optimized at the B3LYP/6-31G(d,p) level in channel 4 (bond length in Å).

(**Z**)-**M3** via (**Z**)-**TS2**, and then the H3′ atom transfers from C2′ atom in (**Z**)-**M3** to C4 atom in (**Z**)-**M4** via (**Z**)-**TS3**. The bond

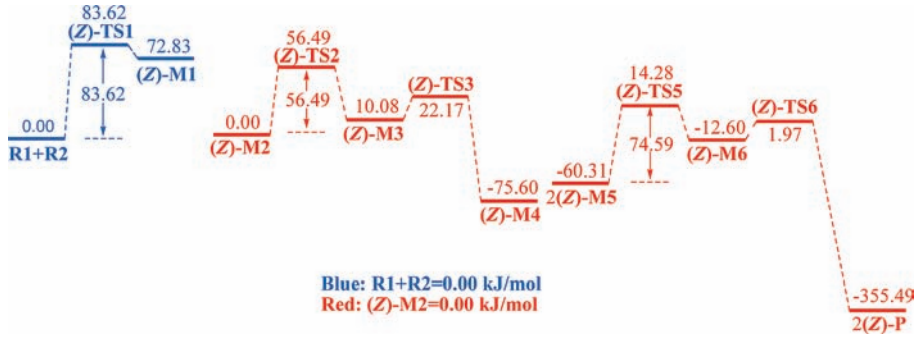

Figure 8. Energy profile of channel 4 (unit: kJ/mol).

TABLE 2: ΔE (Energy Barriers) between the Stationary Points at B3LYP/6-31G(d,p) Level in Different Solvent Using PCM Method (unit: kJ/mol)

	$\Delta E_{\text{Gas-phase}}$	ΔE_{Water}	$\Delta E_{\text{Ethanol}}$	ΔE_{DMSO}	ΔE_{THF}	ΔE_{CCl4}
(*E*)-TS1-(R1+R2)	101.47	84.22	85.23	86.04	88.29	93.87
(*E*)-TS2-(*E*)-M1	35.82	67.44	65.73	57.71	54.17	45.87
(*E*)-TS3-(*E*)-M2	163.29	155.39	156.04	156.26	157.40	160.09
(*E*)-TS4-2(*E*)-M2	89.25	110.63	110.61	103.95	101.50	96.12
(*E*)-TS5-(*E*)-M3	28.52	12.43	12.20	15.08	17.14	22.30
(*Z*)-TS1-(R1+R2)	83.62	70.97	72.21	74.01	75.64	79.29
(*Z*)-TS2-(*Z*)-M2	56.49	39.13	40.38	40.12	42.89	49.22
(*Z*)-TS3-(*Z*)-M3	12.09	1.51	2.35	1.62	2.99	6.90
(*Z*)-TS4-(*Z*)-M5	146.16	155.41	154.23	152.68	151.52	148.99
(*Z*)-TS5-2(*Z*)-M5	74.59	103.81	104.72	95.29	91.90	84.01
(*Z*)-TS6-(*Z*)-M6	14.57	10.54	8.52	9.30	9.70	12.40

lengths of C2−H3 and H3−C4′ are 1.437 and 1.374 Å in (*Z*)-**TS2**, and bond lengths of C2′−H3′ and H3′−C4 are 1.237 and 1.611 Å in (*Z*)-**TS3**, respectively. In addition, the distances of C2−H3 and C2′−H3′ are 2.823 and 2.707 Å in (*Z*)-**M4**, which demonstrates that (*Z*)-**M4** can easily divide into two carbene intermediate (*Z*)-**M5**. The IRC results of (*Z*)-**TS2** and(*Z*)-**TS3** have been provided in the Supporting Information.

It is noteworthy that the highest energy barrier of the proton transfer process is only 56.49 kJ/mol (Figure 6), so the (*Z*)-isomer proton transfer process we suggested should be reasonable at room temperature.

The last step of reaction channel 3 is a three-membered ring rearrangement process as well as channel 1. The bond lengths of N1−C5 and C2−C5 are 1.581 and 1.710 Å in (*Z*)-**TS4**, so we can see that the N1−C5 bond in (*Z*)-**M5** breaks and the C2−C5 bond in (*Z*)-**P** is generated via (*Z*)-**TS4**. Moreover, the dihedral angel of C6−C5−C4−C7 is −170.70° in (*Z*)-**P**, which indicates that the (*Z*)-isomer does not change to (*E*)-isomer in the rearrangement process. Although the energy barrier of this step (146.16 kJ/mol) is 17.13 kJ/mol lower than that of the (*E*)-isomer three-membered ring rearrangement step (163.29 kJ/mol), it is still too high to react at room temperature, which is also mainly due to the strain in the formed three-membered ring in (*E*)-**TS3**.

2.2. Reaction Channel 4. The first step and second proton transfer process of reaction channel 4 (Scheme 3) are the same with reaction channel 3; however, the last rearrangement process is different from reaction channel 3, which is similar to reaction channel 2 and is also a stepwise six-membered ring rearrangement process (Figure 7).

There are two (*Z*)-**M5** to participate in the reaction, the C2−C5′ bond forms in (*Z*)-**M6** via (*Z*)-**TS5** rather than the C2−C5 bond, then the C1−C5 bond and the C1′−C5′ bond break and the C2′-C5 bond generates, and (*Z*)-**M6** rearranges to two (*Z*)-**P** via (*Z*)-**TS6**. The distance of C2−C5′ changes from 1.959 Å in (*Z*)-**TS5** to 1.554 Å in (*Z*)-**M6**, and then the distance of C2′ and C5 changes from 3.118 Å in (*Z*)-**M6** to 2.230 Å in (*Z*)-**TS6**; at last, both of them are 1.469 Å and the six-membered ring breaks to two (*Z*)-**P**.

We set the energy of (*Z*)-**M2** as 0.00 kJ/mol as a reference in the last two processes in reaction channel 4, and the highest energy barrier of the last process is only 74.59 kJ/mol (Figure 8), which is 14.66 kJ/mol lower than that of reaction channel 2 (89.25 kJ/mol); thus, reaction channel 4 is more energetically favorable than the other three channels. Furthermore, the energy of product (*Z*)-**P** is 5.29 kJ/mol lower than that of (*E*)-**P**; it provides additional evidence that the reaction must tend to generate more (*Z*)-product, which is in good agreement with the experimental results. In addition, the highest energy barrier of channel 4 is only 83.62 kJ/mol (Figure 8), it is not a high barrier for the room temperature.

Moreover, solvation effects were considered using PCM as implemented with the water, ethanol, DMSO, THF, and CCl_4 solvents. We have summarized the ΔE of all the reaction channels in the gas phase and different solvents in Table 2. As can be seen from Table 2, the ΔE in red are the energy barriers of the four different rearrangement processes in the four reaction channels. It is noteworthy that ΔE of the rearrangement process in channel 4 is also the lowest energy barrier in the solvents, and $\Delta E_{\text{Gas-phase}}$ values of the rearrangement process in channel 4 are lower than

the ΔE in all the chosen solvents; thus, we think the calculated results can be in good agreement with the experimental results.

Conclusions

This article studies four reaction channels of stereoselective C(2)-vinylation of 1-methylimidazole with 3-phenyl-2-propynenitrile using density functional theory (DFT). The results reveal that this reaction takes place via three processes: initially, the 1-methylimidazole **R1** forms one new bond with electron-deficient alkyne **R2** and the (*E*)- and (*Z*)-isomer zwitterions generate. Simultaneously, from the energy profiles of this step, we can come to a conclusion that the channels corresponding to (*Z*)-isomer zwitterionic intermediate (***Z***)-**M1** (channel 3 and channel 4) are significantly more energetically favorable than the others involving (*E*)-isomer intermediate (***E***)-**M1** (channel 1 and channel 2). The second step is a proton transfer process; all the energy barriers of this process are very low in the four possible channels, so it should be a fast process. In the last rearrangement process, for both the three-membered ring and the six-membered ring rearrangement, the (*Z*)-isomer reaction channels (channels 3 and 4) are more energetically favorable than the (*E*)-isomer channels (channels 1 and 2). Moreover, both energy barriers of the three-membered ring rearrangement are so high at room temperature that channels 1 and 3 may be impossible. The calculations of solvation effects also indicate that channel 4 has the lowest energy barrier in the gas phase.

We conclude that reaction channel 4 is best among all the reaction channels, and the (*Z*)-product is the main product, which agrees with experimental results very well. In addition, as shown by the energy profiles of channel 2 and channel 4 (Figure 4 and Figure 8), both energy barriers of the first steps are the highest energy barrier in each reaction channel; thus, the (***E***)**-TS1** and (***Z***)**-TS1**, which are the transition structures of the first steps in reaction channels, are key for the stereoselectivity of vinylation.

Acknowledgment. The work described in this paper was supported by the National Natural Science Foundation of China (no. 20672104).

Supporting Information Available: Cartesian atomic coordinates and the ZPE (zero-point energies), *E* (electronic energies), *E′* (sum of electronic and zero-point energies), *H* (sum of electronic and thermal enthalpies), *G* (sum of electronic and thermal free energies) of the reactants, intermediates, transition states, and products obtained at the B3LYP/6-31G(d,p) level. The single-point energies of all the optimized stationary points have been computed in the solvents, e.g., water, ethanol, DMSO, THF, and CCl_4 at the B3LYP/6-31G(d,p) level using PCM. In addition, the IRC results of (***Z***)**-TS2** and (***Z***)**-TS3** have been provided. This material is available free of charge via the Internet at http://pubs.acs.org.

References and Notes

(1) Trofimov, B. A.; Andriyankova, L. V.; Belyaeva, K. V.; Mal'kina, A. G.; Nikitina, L. P.; Afonin, A. V.; Ushakov, I. A. *J. Org. Chem.* **2008**, *73*, 9155–9157.

(2) (a) Grimmett, M. R. *Comprehensive Heterocyclic Chemistry II*; Katritsky, A. R., Scriven, E. F. V., Eds.; Pergamon: Oxford, 1966; Vol. 3, pp 77−220. (b) Bellina, F.; Cauteruccio, S.; Rossi, R. *Tetrahedron* **2007**, *63*, 4571–4624.

(3) De Luca, L. *Curr. Med. Chem.* **2006**, *13*, 1–23.

(4) Sennequier, N.; Wolan, D.; Stuehr, D. *J. Biol. Chem.* **1999**, *274*, 930–938.

(5) (a) Mano, T.; Stevens, R. W.; Ando, K.; Nakao, K.; Okumura, Y.; Sakakibara, M.; Okumura, T.; Tamura, T.; Miyamoto, K. *Bioorg. Med. Chem.* **2003**, *11*, 3879–3887. (b) Mano, T.; Okumura, Y.; Sakakibara, M.; Okumura, T.; Tamura, T.; Miyamoto, K.; Stevens, R. W. *J. Med. Chem.* **2004**, *47*, 720–725.

(6) Dyck, B.; Goodfellow, V. S.; Philips, T.; Grey, J.; Haddach, M.; Rowbotton, M.; Naeve, G. S.; Brown, B.; Saunders, J. *Bioorg. Med. Chem. Lett.* **2004**, *10*, 1151–1154.

(7) Kiselyov, A. S.; Semenova, M.; Semenov, V. V. *Bioorg. Med. Chem. Lett.* **2006**, *16*, 1440–1444.

(8) Blum, C. A.; Zheng, X.; De Lombaert, S. *J. Med. Chem.* **2004**, *47*, 2318–2325.

(9) Ding, H.; Ma, C.; Yang, Y.; Wang, Y. *Org. Lett.* **2005**, *7*, 2125–2127.

(10) Di Santo, R. D.; Tafi, A.; Costi, R.; Botta, M.; Artico, M.; Corelli, F.; Forte, M.; Caporuscio, F.; Angiolella, L.; Palamara, A. T. *J. Med. Chem.* **2005**, *48*, 5140–5153.

(11) Zhao, Z. Y.; McLeod, A.; Harusawa, S.; Araki, L.; Yamaguchi, M.; Kurihara, T.; Lilley, D. M. J. *J. Am. Chem. Soc.* **2005**, *127*, 5026–5027.

(12) Oxley, J. D.; Prozorov, T.; Suslick, K. S. *J. Am. Chem. Soc.* **2003**, *125*, 11138–11139.

(13) Kanazawa, C.; Kamijo, S.; Yamamoto, Y. *J. Am. Chem. Soc.* **2006**, *128*, 10662–10663.

(14) (a) Welton, T. *Chem. Rev.* **1999**, *99*, 2071–2083. (b) Rahman, T.; Fukuyama, T.; Ryu, I.; Suzuki, K.; Yonemura, K.; Hughes, P. F.; Nokihara, K. *Tetrahedron Lett.* **2006**, *47*, 2703–2706. (c) Xu, J.-M.; Liu, B.-K.; Wu, W.-B.; Qian, C.; Wu, Q.; Lin, X.-F. *J. Org. Chem.* **2006**, *71*, 3991–3993.

(15) (a) Bourissou, D.; Guerret, O.; Gabai, F. P.; Bertrand, G. *Chem. Rev.* **2000**, *100*, 39–91. (b) Nair, V.; Rajesh, C.; Vinod, A. U.; Bindu, S.; Sreekanth, A. R.; Mathen, J. S.; Balagopal, L. *Acc. Chem. Res.* **2003**, *36*, 899–907. (c) Nair, V.; Menon, R. S.; Sreekanth, A. R.; Abhilash, N.; Biju, A. T. *Acc. Chem. Res.* **2006**, *39*, 520–530. (d) Marion, N.; Diez-Gonzalez, S.; Nolan, S. P. *Angew. Chem.* **2007**, *46*, 2988–3000.

(16) Chen, W.; Zhang, Y. Y.; Zhu, L. B.; Lan, J. B.; Xie, R. G.; You, J. S. *J. Am. Chem. Soc.* **2007**, *129*, 13879–13886.

(17) Park, S.; Kwon, O.-H.; Kim, S.; Park, S.; Choi, M.-G.; Cha, M.; Park, S. Y.; Jang, D.-J. *J. Am. Chem. Soc.* **2005**, *127*, 10070–10074.

(18) Miranda-Soto, V.; Grotjahn, D. B.; DiPasquale, A. G.; Rheingold, A. L. *J. Am. Chem. Soc.* **2008**, *130*, 13200–13201.

(19) Choudary, B. M.; Sridhar, C.; Kantam, M. L.; Venkanna, G. T.; Sreedhar, B. *J. Am. Chem. Soc.* **2005**, *127*, 9948–9949.

(20) McNab, H.; Thornley, C. *J. Chem. Soc., Perkin Trans. 1* **1997**, *15*, 2203–2209.

(21) Williams, D. R.; Lee, M.-R.; Song, Y.-A.; Ko, S.-K.; Kim, G.-H.; Shin, I. *J. Am. Chem. Soc.* **2007**, *129*, 9258–9259.

(22) Gusarova, N. K.; Arbuzova, S. N.; Reutskaya, A. M.; Ivanova, N. I.; Baikalova, L. V.; Sinegovskaya, L. M.; Chipanina, N. N.; Afonin, A. V.; Zyryanova, I. A. *Chem. Heterocycl. Compd.* **2002**, *38*, 65–70.

(23) Karthikeyan, S.; Potisek, S. L.; Piermattei, A.; Sijbesma, R. P. *J. Am. Chem. Soc.* **2008**, *130*, 14968–14969.

(24) Trofimov, B. A.; Tarasova, O. A.; Shemetova, M. A.; Afonin, A. V.; Klyba, L. V.; Baikalova, L. V.; Mikhaleva, A. I. *Zh. Org. Khim.* **2003**, *39*, 408–414.

(25) Sparks, R. B.; Combs, A. P. *Org. Lett.* **2004**, *6*, 2473–2475.

(26) Trofimov, B. A.; Andriyankova, L. V.; Zhivet'ev, S. A.; Mal'kina, A. G.; Voronov, V. K. *Tetrahedron Lett.* **2002**, *43*, 1093–1096.

(27) Trofimov, B. A.; Andriyankova, L. V.; Shaikhudinova, S. I.; Kazantseva, T. I.; Mal'kina, A. G.; Afonin, A. V. *Synthesis* **2002**, *7*, 853–855.

(28) Andriyankova, L. V.; Mal'kina, A. G.; Afonin, A. V.; Trofimov, B. A. *Mendeleev Commun.* **2003**, *4*, 186–188.

(29) Andriyankova, L. V.; Mal'kina, A. G.; Nikitina, L. P.; Belyaeva, K. V.; Ushakov, I. A.; Afonin, A. V.; Nikitin, M. V.; Trofimov, B. A. *Tetrahedron* **2005**, *61*, 8031–8034.

(30) Trofimov, B. A.; Andriyankova, L. V.; Tlegenov, R. T.; Mal'kina, A. G.; Afonin, A. V.; Il'icheva, L. N.; Nikitina, L. P. *Mendeleev Commun.* **2005**, *1*, 33–35.

(31) Trofimov, B. A.; Andriyankova, L. V.; Mal'kina, A. G.; Belyaeva, K. V.; Nikitina, L. P.; Dyachenko, O. A.; Kazheva, O. N.; Chekhlov, A. N.; Shilov, G. V.; Afonin, A. V.; Ushakov, I. A.; Baikalova, L. V. *Eur. J. Org. Chem.* **2007**, *6*, 1018–1025.

(32) (a) Moles, P.; Oliva, M.; Safont, V. S. *J. Phys. Chem. A* **2006**, *110*, 7144–7158. (b) Montero-Campillo, M. M.; Rodríguez-Otero, J.; Cabaleiro-Lago, E. *J. Phys. Chem. A* **2008**, *112*, 2423–2427. (c) Johnson, L. E.; DuPré, D. B. *J. Phys. Chem. A* **2007**, *111*, 11066–11073. (d) Okovytyy, S. I.; Sviatenko, L. K.; Gaponov, A. O.; Tarabara, I. N.; Kasyan, L. I.; Leszczynski, J. *J. Phys. Chem. A* **2009**, *113*, 1475–1480. (e) Galabov, B.; Atanasov, Y.; Ilieva, S.; Schaefer, H. F. *J. Phys. Chem. A* **2005**, *109*, 11470–11474. (f) Kınal, A.; Piecuch, P. *J. Phys. Chem. A* **2006**, *110*, 367–378. (g) Wei, D.-h.; Tang, M.-s.; Zhao, J.; Sun, L.; Zhang, W.-j.; Zhao, C.-f.; Zhang, S.-r.; Wang, H.-m. *Tetrahedron: Asymmetry* **2009**, *20*, 1020–1026.

(33) Frisch, M. J.; Trucks, G. W.; Schlegel, H. B.; Scuseria, G. E.; Robb, M. A.; Cheeseman, J. R.; Montgomery, J. A.; Vreven, T., Jr.; Kudin, K. N.; Burant, J. C.; Millam, J. M.; Iyengar, S. S.; Tomasi, J.; Barone, V.; Mennucci, B.; Cossi, M.; Scalmani, G.; Rega, N.; Petersson, G. A.; Nakatsuji, H.; Hada, M.; Ehara, M.; Toyota, K.; Fukuda, R.; Hasegawa, J.; Ishida, M.; Nakajima, T.; Honda, Y.; Kitao, O.; Nakai, H.; Klene, M.; Li,

X.; Knox, J. E.; Hratchian, H. P.; Cross, J. B.; Bakken, V.; Adamo, C.; Jaramillo, J.; Gomperts, R.; Stratmann, R. E.; Yazyev, O.; Austin, A. J.; Cammi, R.; Pomelli, C.; Ochterski, J. W.; Ayala, P. Y.; Morokuma, K.; Voth, G. A.; Salvador, P.; Dannenberg, J. J.; Zakrzewski, V. G.; Dapprich, S.; Daniels, A. D.; Strain, M. C.; Farkas, O.; Malick, D. K.; Rabuck, A. D.; Raghavachari, K.; Foresman, J. B.; Ortiz, J. V.; Cui, Q.; Baboul, A. G.; Clifford, S.; Cioslowski, J.; Stefanov, B. B.; Liu, G.; Liashenko, A.; Piskorz, P.; Komaromi, I.; Martin, R. L.; Fox, D. J.; Keith, T.; Al-Laham, M. A.; Peng, C. Y.; Nanayakkara, A.; Challacombe, M.; Gill, P. M. W.; Johnson, B.; Chen, W.; Wong, M. W.; Gonzalez, C.; Pople, J. A. *Gaussian 03*, revision C.02; Gaussian, Inc., Wallingford, CT, 2004.

(34) Becke, A. D. *J. Chem. Phys.* **1993**, *98*, 5648–5652.
(35) Lee, C.; Yang, W.; Parr, R. G. *Phys. Rev. B* **1988**, *37*, 785–789.
(36) Gonzalez, C.; Schlegel, H. B. *J. Chem. Phys.* **1989**, *90*, 2154–2161.
(37) Gonzalez, C.; Schlegel, H. B. *J. Phys. Chem.* **1990**, *94*, 5523–5527.
(38) Barone, V.; Cossi, M. *J. Phys. Chem. A* **1998**, *102*, 1995–2001.
(39) Mennucci, B.; Tomasi, J. *J. Chem. Phys.* **1997**, *106*, 5151–5158.

JP9047874